ELECTRONICS AND ELECTRICAL ENGINEERING
ISSN 1392 – 1215 *2012. No. 5(121)*
ELEKTRONIKA IR ELEKTROTECHNIKA

T 125 *AUTOMATION, ROBOTICS*
AUTOMATIZAVIMAS, ROBOTECHNIKA

Computational Fluid Dynamics (CFD) Investigations of the Effect of Placing a Metallic Mesh in the Channels of a Passive Solar Collector Model

G. Iordanou, G. Tsirigotis
Dept. of Electrical Engineering, Div. of Electronics & Control Systems, Kavala Institute of Technology, 65404, Agios Loukas, Kavala, Greece, phone: +302510 46226, e-mails: greor@msn.com, tsirigo@teikav.edu.gr

crossref http://dx.doi.org/10.5755/j01.eee.121.5.993

Introduction

Numerous investigations in to solar thermosyphon systems have been conducted, but they are limited to a small range of heat exchanger configurations, flow visualisation and heat transfer. CFD models are even fewer in the case of flat-plate solar water collectors. The majority of the initial investigations were based on a model developed by Duffie and Beckman for flat plate solar collectors. Tests on solar collectors under varying conditions over time have been presented using relations that give the characteristics of the collector by a Fourier transform of differential equations [1, 2]. Attempts had been made to develop models that describe the physical and geometrical complexity of the system more accurately. The total daily energy yield predicted by the models for a number of days of different weather conditions was calculated using a reference collector parameter set [3]. These models are currently being used by common simulation software packages such as TRNSYS and T-Sol 2.0. Recently a one-dimensional transient numerical model for flat plate solar thermal devices was developed following virtual testing procedures in accordance with the experimental test methods described by European and International standards [4].

Other theoretical investigations focused on vertical mantle tanks for solar domestic hot water systems. Differently designed mantle tanks have been evaluated using a transient three-dimensional CFD-model (CFX 4.1) [5, 6]. A three-dimensional numerical model was developed using the CFD numerical package FLUENT to evaluate the flow patterns in the annular passageways and the heat transfer into the inner tank of a solar water system. Flow visualization was used to investigate the flow structure. [7]. A first approach to numerically examine Integrated Collector Systems was conducted by using a two and three-dimensional CFD model utilising the CFD-code FLUENT, neglecting the heat exchanger presence.

The flow field inside the storage was examined using various turbulence models [8]. Two 3D numerical models were developed using the CFD package FLUENT 6.1. The first model was developed neglecting the heat exchanger. presence of the heat exchanger was taken into account in the second model. All turbulence mode available in FLUENT were tested and the k-ω model was the most appropriate. Studies of cavities has been broadened by variations that include different geometries, such as the effect of curved walls, addition of partitions and changes in the boundary conditions, such as spatially varying temperatures [9].Testing showed that the flow rising along the hot wall joins the flow descending down the cold wall and vice versa to make a complete loop along the walls. [10].

Mesh size is critical for the CFD analysis, especially when dealing with natural convection [11]. This investigation found that the calculated convective heat transfer depends on the size of the grids by analyzing laminar flows of forced and natural convection over a flat plate. Two-dimensional convective flows in shallow cavities with conducting horizontal boundaries and driven by differential heating of the two vertical end walls, were studied numerically over a range of Rayleigh numbers and Prandtl numbers. It was observed that the aspect ratio is the most important parameter affecting the heat and fluid flow and that higher heat transfer rate is obtained at lower aspect ratio for a certain value of Grashof number [12]. In natural convection heat transfer in porous enclosures, indicated that local Nusselt numbers are very sensitive to thermal stratification [13]. Extensive computations presented for a wide range of wave amplitudes and phases, and some global heat transfer rates were given. Two collectors were compared; one that had a wavy absorber and a second that had a flat absorber. Commercial software was used to simulate the laminar flow and thermal field.

Natural convection heat transfer and fluid flow was strongly affected by the shape and inclination angle of thecollector [14, 15].

Simulation work

CFD modelling of a simplified solar collector was investigated by placing a metallic mesh inside the pipe of a passive system (free convection) which represented a segment of the solar collector operating in similar conditions. This was carried out by employing CFD commercial software FLUENT which uses the control volume numerical technique for solving the governing equations of flow and heat transfer. Fig. 1 illustrates the design used in CFD numerical investigations.

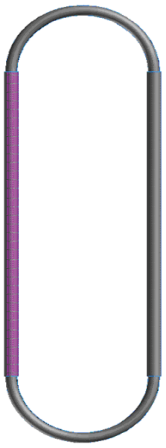

Fig. 1. Designed geometry

The model consisted of two vertical sections made of cylindrical pipes connected at the top and bottom parts with adiabatic curved pipes to form the enclosed loop. The pipes on the left and right were used for heating and cooling the fluid, respectively.

The model geometry is 350 mm high and the external diameter of the pipes and the thickness of pipe walls are 10 and 1 mm, respectively. Two cases were investigated, namely with and without metallic mesh being placed inside the heating pipe. The full geometry and computational mesh for CFD simulations were created in the Gambit software, which is used as a pre-processor for the CFD solver and post-processor, namely FLUENT.

Fig. 2 shows the geometry of the heating vertical pipe with the metallic mesh placed inside. The physical dimensions used to closely reflect the real geometry of the metallic mesh shown in Fig. 3.

A time consuming process while designing the proposed geometry was the creation and later meshing of the volume of water within the netted pipe. This was due to the large number of rectangles created at the internal surface of the pipe because of the presence of the net. It was found that the rational number of hexahedral control volumes providing acceptable level of accuracy was about 27,000. Such a mesh was created by applying Quad-Map meshing scheme. The meshing element-scheme combination used for meshing the whole domain was Hex/Wedge – Cooper. The complete meshed volume water for the section of the heating tube is illustrated below (Fig 4). Using similar technique the “solid” domain was meshed including the volume of all pipes and that of the metallic mesh.

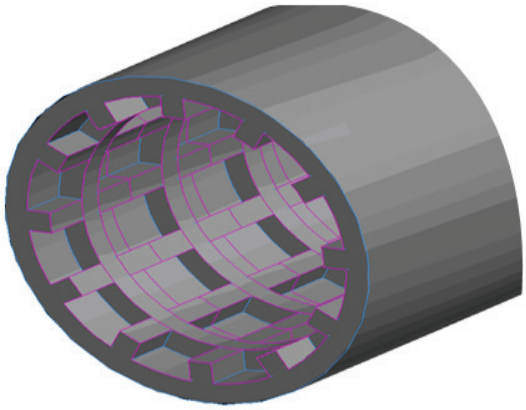

Fig. 2. 3D geometry of the heating pipe

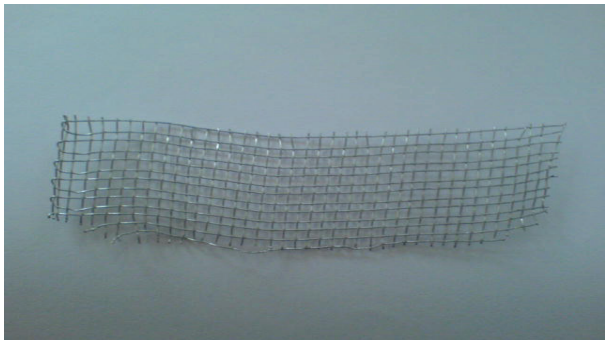

Fig. 3. Aluminium mesh

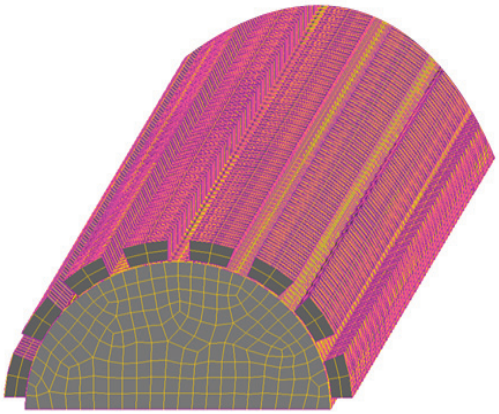

Fig. 4. Computational mesh for the water domain

Since the symmetry plane has been used to halve the computational grid, the flow, temperature and pressure gradients were set to be zero on this plane as it is illustrated in Fig. 5. It was mentioned above that the total number of mesh cells created in the entire geometry was about 27.000 with the density of the grid being greater in areas of large temperature and velocity gradients. Grid sensitivity tests (trial and approach) showed a variation of about 1% in the solution when the size of volumes increased or decreased by 10%.

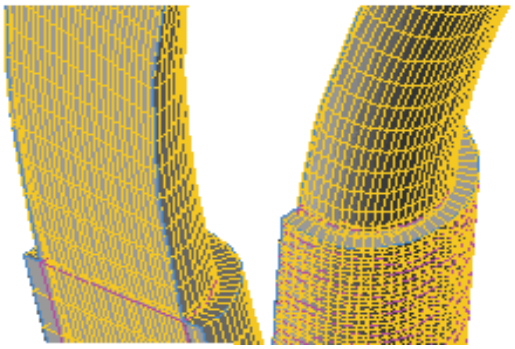

Fig. 5. Sections of the meshed grid

Simulation results

The properties of water were temperature-dependent and polynomial piecewise-linear functions were used to take into account the above dependence of water properties upon its temperature. On the outer surface of the heating and cooling tubes the heat fluxes equivalent to 905 W/m^2 and – 905 W/m^2 respectively, were specified in order to induce the free convection flow. The effect of gravity was taken into account along the vertical axis by specifying the negative acceleration value of 5.62 m/s^2 (cosine of 55^o multiplied by the gravitational forces constant) since the solar collectors was assumed to be inclined. The inclination angle was set to 55^o which is the latitude of Durham, U.K. The total computational time for both cases was about 35 minutes as the system reached a steady state where the plotted residuals did not vary any longer. At this moment results could be observed and analysed accordingly.

Fig. 6 presents the temperature contours for both the cases when steady-state operational conditions were achieved.

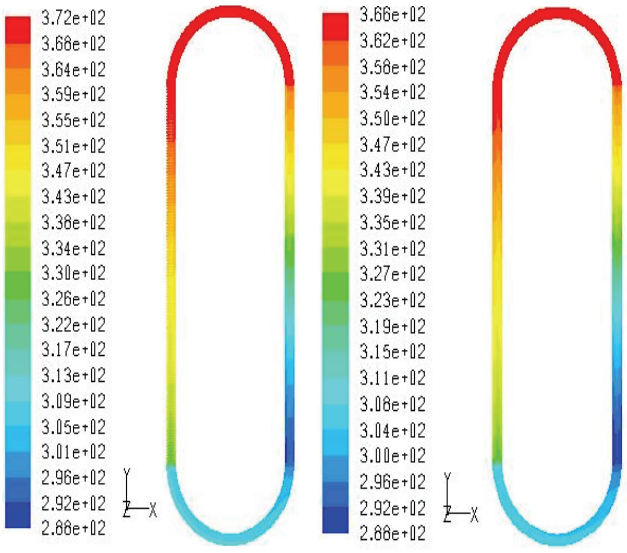

Fig. 6. Temperature contours of both geometries (K)

The numerical results obtained, clearly demonstrate that the proposed design of the solar collector provides a considerable performance improvement. In both cases, the identical boundary and initial conditions were applied as described before. The left image in Fig. 6 shows results for the simplified collector with the mesh insertion, while the right image presents the temperature contours for the conventional collector. It can be seen that the working fluid is heated to the temperature 372 K which is 6 degrees higher compared to the maximum water temperature in the conventional solar collector. Considering the relatively small dimensions of both collectors the increase in temperature is quite significant. On the outer surface of the heating and cooling tubes the heat fluxes were equivalent to 905 W/m^2 and -905 W/m^2 respectively. The power output Q of the designed collector with the metal mesh and the conventional was 78 W and 75 W respectively. A graphical representation of the temperature rise in K along the length of the heating tube is shown in Fig. 7. The temperature T1 (blue line) refers to the case with the mesh insertion and it can be seen that for such design, the temperature increase in the heating tube is higher all along its length compared to that of a conventional collector displayed by the red line T2.

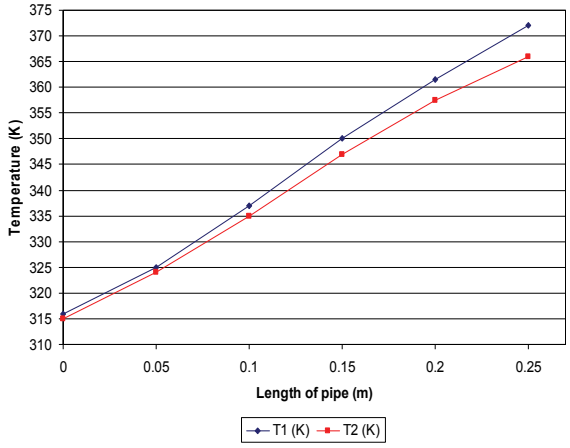

Fig. 7. Temperature variation through the heating pipes

The variation of the water temperature in the section of the heating tube along its radius is demonstrated in Fig. 8 and it can be seen that the thickness of the near-wall layer of the fluid (water) or zone which has the high temperature is considerably greater for the case of the collector with metallic mesh insertion (image on the left). The variation of the water temperature in the cooling tube along its radius is demonstrated in Fig. 9. In the case of the conventional collector (image on the right) there is a domination of the lower temperature zone in the centre of the heating tube since the water entering has a lower temperature.

The flow in the collector was induced by the density gradient, which in turn was caused by the heating and cooling the working fluid. In both cases very similar patterns were obtained. For the given boundary conditions the density of water changes from 962.6 kg/ m^3 after heating process to 999 kg/ m^3 where the temperature is the lowest. In the design with the metal insertion case it varies between 958 kg/ m^3 to 998 kg/ m^3. Also from numerical results the water is cooled down more in the conventional design since higher water density results to a lower water temperature at the cooling tube.

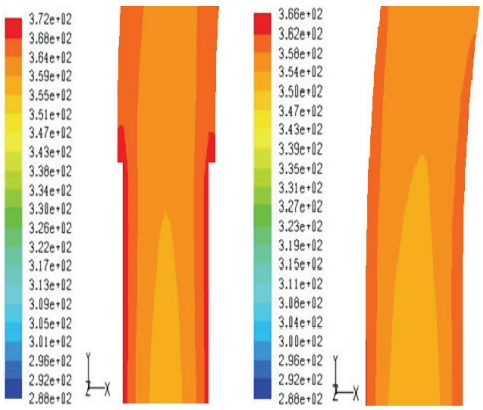

Fig. 8. Temperature contours at exit of the hot region

Results indicated that flow remains laminar in both cases though there was a small increase in the velocity at the centre of the heating pipe of the collector with metallic insertion, (does not exceed the velocity of the conventional design), due to the reduction in the cross-sectional area. At the pipe walls the velocity drops due to friction from the metallic insertion resulting to an overall velocity reduction along the pipe. The overall velocity then drops at the centre of the pipe after passing the zone where the metallic. Due to the layer-by-layer motion the heat was transferred at a slower rate from the near wall zone in the direction toward the axis of the tube.

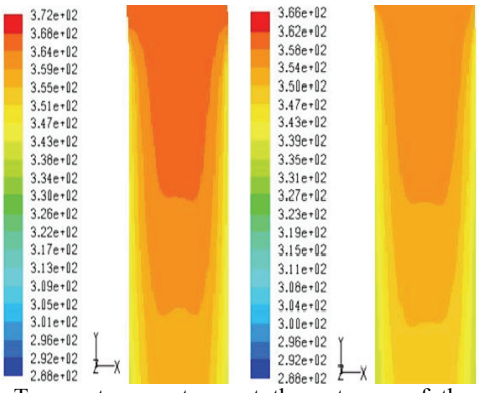

Fig. 9. Temperature contours at the entrance of the cooling region

The overall velocity flow rate is higher in the conventional scheme having 4.7 10^{-3} m/sec compared to 4.4 10^{-3} m/sec in the system with the metallic mesh. In order to validate the simulation findings it was essential to relate them to literature and hence expression (1) was used which is valid for constant surface heat flux. The output temperatures T_{out1} and T_{out2} were obtained for the collector with the metal insertion and the convectional collector, respectively. Data from the simulations was used in order to determine the output temperatures

$$T_{out} = \frac{Q \cdot P}{\left(\dot{m} \cdot C_p\right)} + T_{ref}, \qquad (1)$$

where Q is the heat flux in W/m^2, P is the perimeter of the pipe in mm, $\dot{m}$ in the mass flow rate in Kg/sec, C_p is the specific heat in J/Kg ^{o}C, T_{out} and T_{ref} are the output and average temperature of the system in ^{o}C, respectively. Table 1 illustrates data obtained from simulation and other parameters from relevant charts i.e. C_p, to evaluate the CFD findings with the literature.

Table 1. Simulation data obtained for both cases

	Collector with metal	**Conventional**
Q(W/m^2)	905	905
P (mm)	31.15	31.15
T_{ref} (^{o}C)	341	336
$\dot{m}$ (	$0.217 \cdot 10^{-3}$	$0.233 \cdot 10^{-3}$
C_p (J/Kg	4190	4185

By placing the data to the expression (1) for the collector with the metallic mesh the output temperature T_{out1} was **372.2 ^{o}C** and for the conventional T_{out2} was **365.6 ^{o}C**. These results showed the accuracy of the CFD model since the values obtained were very close to the simulation ones **372 ^{o}C** and **366 ^{o}C** respectively (shown in Figure 3.a).

The pressure drop in the heating pipe for the given boundary conditions in both cases was relatively small, being about 3 and 7 Pa for the conventional design and the design with the metallic mesh insertion, respectively. Such low values of the pressure drop do not affect significantly the flow rates of the fluid and did not affect thermal performance of the both solar collectors. The operation of two geometries of the solar collector was CFD modelled as a function of the heat flux values on the heating and cooling tubes between 610 W/m^2 to 1070 W/m^2. The average heat transfer coefficient from solid domain to fluid in the heating pipe was determined from CFD simulations, see Table 2.

Fluent uses the relation (2) shown below in order to calculate the heat transfer coefficient of the examined geometry

$$h = \frac{Q}{\left(T_w - T_{ref}\right)}, \qquad (2)$$

where Q is the heat flux in W/m^2, T_w and T_{ref} are the temperature of the wall and a reference temperature, respectively. It can be observed that the heat transfer value in the case of the collector with the metallic insertion was noticeably higher and the difference in heat transfer coefficients rises with increase of the heat flux applied.

Further using results from CFD calculations the Rayleigh number (Ra) was determined, which is a measure of the strength of the heat transfer due to natural convection at the examined geometries.

Table 2. Heat transfer coefficients (h) of the examined cases

Heat Flux (W/ m^2)	***h* Porous Case (W/m^2 K)**	***h* Conventional Case (W/m^2 K)**
1070	207.67	194.83
905	171.82	160.20
750	134.40	122.10
610	115.60	99.00

Using CFD simulations the heat transfer correlation was derived for different values of the heat flux applied on the surfaces of heating and cooling tubes. Two different

heat fluxes were used (1070 W/m^2 and 610 W/m^2) in order to accomplish this task. The Rayleigh number (*Ra*) is defined as

$$Ra = \frac{g\beta\Delta TL^3}{\nu\alpha}, \quad (3)$$

where β is the thermal expansion coefficient; L the length of the pipe, ν the kinematic viscosity and α is the thermal diffusivity. The values of the (3) automatically change according to the change of temperature during the simulation process apart from the length L that remains constant. The range of *Ra* Number obtained in both cases suggested that the natural convection was the dominant mode of heat transfer. The heat transfer correlation relating Nusselt (*Nu*) and Rayleigh (*Ra*) numbers was sought in the following form

$$Nu = c(Ra)^n, \quad (4)$$

where c is the constant of proportionality and n is a variable determined by conditions on the constant heat flux surfaces or isothermal surfaces. This n coefficient was calculated and its average was used to calculate c. The two parameters c and n were calculated by coupling equations in pairs as shown below:

$$Nu_1 = c(Ra_1)^n, \quad (5)$$

$$Nu_2 = c(Ra_2)^n, \quad (6)$$

$$n = \log_{\frac{Ra2}{Ra1}} \frac{Nu_2}{Nu_1}. \quad (7)$$

The n parameter was calculated for a range of *Ra* and *Nu* numbers as varied along the characteristic pipe length and its average was used to calculate c.

The final correlation derived was for the heat fluxes of 1070 W/m^2 and 610 W/m^2 respectively:

$$Nu_{(1070)} = 0.013(Ra)^{0.285}, \quad (8)$$

$$Nu_{(610)} = 0.007(Ra)^{0.285}. \quad (9)$$

The value of n=0.285 suggested that conditions close to the isothermal ones were present on the surface of the geometry [16]. After the numerical solution was converged reaching the steady state and due to the presence of the aluminium mesh insertion it could be interpreted that the heat transferred to the fluid was uniform. Equations (8) and (9) can be used to derive the *Nu* number in relation to *Ra* number under constant heat flux (from 610 W/m^2 to 1000 W/m^2). Also these two relations can be used to obtain other useful parameters that can predict the performance of a collector i.e. heat transfer coefficient h. Collectors are formed by individual tubes and therefore the above derived correlations can be applied to real systems to examine each of the collector's pipes individually over a characteristic length. The values obtained from Fluent and those calculated from the correlations derived are listed in the Table 3.

Table 3. *Nu* and *Ra* Number relation

1070 W/m^2			**610 W/m^2**		
Ra	***Nu***	***Nu calculated***	***Ra***	***Nu***	***Nu calculated***
2.5E+09	6.3	6.3	2E+09	3.3	3.1
5E+09	7.5	7.6	4E+09	4.0	3.8
7.5E+09	8.5	8.5	5E+09	4.3	4.0
1E+10	9.3	9.2	8E+09	4.5	4.6
1.5E+10	10.0	10.3	1.2E+10	4.8	5.1
Average values					
Ra	***Nu***	***Nu calculated***	***Ra***	***Nu***	***Nu calculated***
8E+09	**8.3**	**8.4**	**6.2E+09**	**4.2**	**4.3**

Results showed that there was a very good agreement between *Nu* numbers obtained both from Fluent and the proposed correlation.

Using the values from Table 3 a graph was plotted shown in Fig. 11.

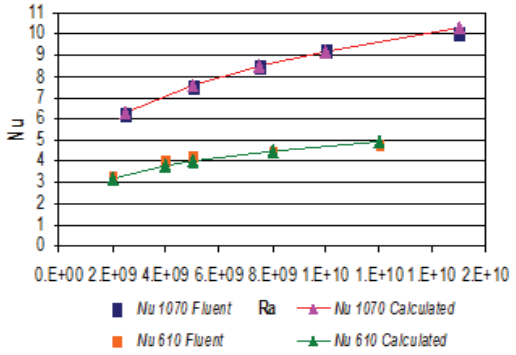

Fig. 10. Rayleigh number as function of nusselt number

It displays the relation between the *Nusselt Number Nu* and the *Raleigh Number Ra*. It also illustrates the difference between the values of the *Nu* number obtained from the derived correlation and those from Fluent. The average *Nu Number* ranges between 4.2 to 8.3 and the *Ra* number between $6.2 \cdot 10^9$ to $8 \cdot 10^9$ for heat fluxes between 610 W/m^2 to 1070 W/m^2 being in the range of the laminar flow. This was chosen to demonstrate the mechanism of the heat transfer intensification due to the presence of the metallic mesh insertion in the pipe.

Conclusions

The analysis of the CFD model results, clearly demonstrated that the application of a metallic mesh insertion in the heating channels of passive solar collectors is an efficient way to intensify heat transfer from the heating surface to the working fluid and consequently improving the thermal performance of solar collectors.

The output temperatures obtained from simulations for the geometry with the metallic mesh and for the conventional were validated with literature which showed the accuracy of the CFD model. Higher output temperature, *Nu* and *Ra*

numbers and finally higher heat transfer coefficient *h* for the model with the metallic mesh compared to convectional, clearly displayed the benefits of using this heat transfer enhancement technique.

From the obtained expressions (8) and (9) the *Nu* number in relation to *Ra* number under constant heat flux (from 610 W/m^2 to 1000 W/m^2) can be derived for a solar water collector's section pipe with a characteristic length of 0.25 m. These two relations can be used to obtain other useful parameters that can predict the performance of a collector i.e. heat transfer coefficient *h*.

References

1. **Kamminga W.** Experiences of a solar collector test method using Fourier transfer functions // International Journal of Heat Mass Transfer, 1995. – Vol. 28. – P. 1393–1404.
2. **Isakson P.** Solar collector model for testing and simulation. – Final report for BFR project Nr. 900280–1. – Building Services Engineering, Royal Institute of Technology, Stockholm, 1995.
3. **Schnieders J.** Comparison of the energy yield predictions of stationary and dynamic solar collector models and the models' accuracy in the description of a vacuum tube collector // Solar Energy, 1997. – Vol. 61. – P. 179–190.
4. **Cadafalch J.** A detailed numerical model for flat plate solar thermal devices // Solar Energy (UPC), 2008.
5. **Shah L. J., Furbo S.** Correlation of experimental and theoretical heat transfer in mantle tanks used in low flow SDHW systems // Solar Energy, 1998. – Vol. 64. – P. 245–256.
6. **Nasr G. L., M. Behnia**. Flow development and heat transfer characteristics in a concentric heat exchanger with application to solar thermosyphon systems // Proceedings 5th Australian Natural Convection Workshop. – Sydney, Australia, 1996. – P. 31–34.
7. **Morrison G. L., Nasr A., Behnia M. and Rosengarten G** Performance of horizontal mantle heat exchangers in solar water heating systems // Proceeding ISES Solar World Congress. – Taejon, Korea, 1997. – P. 149–158.
8. **Gertzos K. P., Caouris Y. G.** Experimental and computational study of the developed flow field in a flat plate integrated collector storage (ICS) solar device with recirculation // Experimental Thermal and Fluid Science 31, 2007. – P. 1133–1145.
9. **Amaresh D., Kumar D. M.** Laminar natural convection in an inclined complicated cavity with spatially variable wall temperature // Int. J Heat Mass Transfer, 2005. – Vol. 48. – P. 3833–3854.
10. **Yang Y.** Laminar natural convective flow in inclined rectangular glazing cavities // CEERE. – University of Massachusetts, Department of Mechanical Engineering and Industrial Engineering, 2002.
11. **Zhai Z., Chen C.** Numerical determination and treatment of convective heat transfer coefficient in coupled building energy simulation // Build Environ, 2004. – Vol. 39. – P. 1001–1009,.
12. **Mahmud S., Das P. K., Hyder N., Islam A. K. M. S.** Free convection heat transfer in an enclosure with vertical wavy walls // International Journal of Thermal Science, 2002. – Vol. 41. – P. 440–446.
13. **Kumar B. V. R.** Natural convection in a thermally stratified wavy vertical porous enclosure // Numerical Heat Transfer, 2003. – Vol. 43. – P. 753–776.
14. **Rees D. A. S., Pop I.** Free convection induced by a horizontal wavy surface in a porous medium // Fluid Dynamics Research, 1994. – Vol. 14. – P. 151–166.
15. **Varola Y., Hakan F., Oztop A.** A comparative numerical study on natural convection in inclined wavy and flat–plate solar collectors // Building and Environment, 2008. – Vol. 43. – P. 1535–1544.
16. **Bejan A.** Convection Heat Transfer. – Wiley, New York, 1993.

Received 2011 12 13
Accepted after revision 2012 01 14

G. Iordanou, G. Tsirigotis. Computational Fluid Dynamics (CFD) Investigations of the Effect of Placing a Metallic Mesh in the Channels of a Passive Solar Collector Model // Electronics and Electrical Engineering. – Kaunas: Technologija, 2012. – No. 5(121). – P. 69–74.

This article is concerned with CFD investigations of the effect of placing a metallic mesh inside the channel of the simplified passive solar collector design. Numerical results obtained demonstrated that such a design would improve the heat transfer from the walls of channels to the liquid and therefore would result in the hot water production capacity of the solar collector. Using numerical models that can predict the physical performance of a design project, it is possible to find, optimised solutions without creating a large and expensive series of models. Ill. 10, bibl. 16, tabl. 3 (in English; abstracts in English and Lithuanian).

G. Iordanou, G. Tsirigotis. Metalinio tinklelio paklojimo į pasyviojo saulės kolektoriaus modelio kanalus efekto skaičiuojamosios hidrodinamikos tyrimai // Elektronika ir elektrotechnika. – Kaunas: Technologija, 2012. – Nr. 5(121). – P. 69–74.

Pateikti skaičiuojamosios hidrodinamikos (SHD) tyrimai vertinat metalinio tinklelio paklojimo į supaprastinto pasyvinio saulės kolektoriaus modelio kanalus efektą. Gauti skaitmeniniai rezultatai parodė, kad toks sprendimas turėtų pagerinti šilumos perdavimą iš kanalo sienelių į skystį ir kartu padidinti saulės kolektoriaus karšto vandens gamybos apimtį. Naudojant skaitmeninius modelius, kurie leidžia nuspėti kuriamos struktūros darbingumą, galima rasti optimizuotus sprendimus nekuriant daugybės fizinių modelių. Il. 10, bibl. 16, lent. 3 (anglų kalba; santraukos anglų ir lietuvių k.).